Supplementary Data

A small ribosome-associated ncRNA globally inhibits translation by restricting ribosome dynamics

Julia Reuther[1,†], Lukas Schneider[1,2,†], Ioan Iacovache[3,†], Andreas Pircher[1,2], Walid H. Gharib[4], Benoît Zuber[3]* and Norbert Polacek[1]*

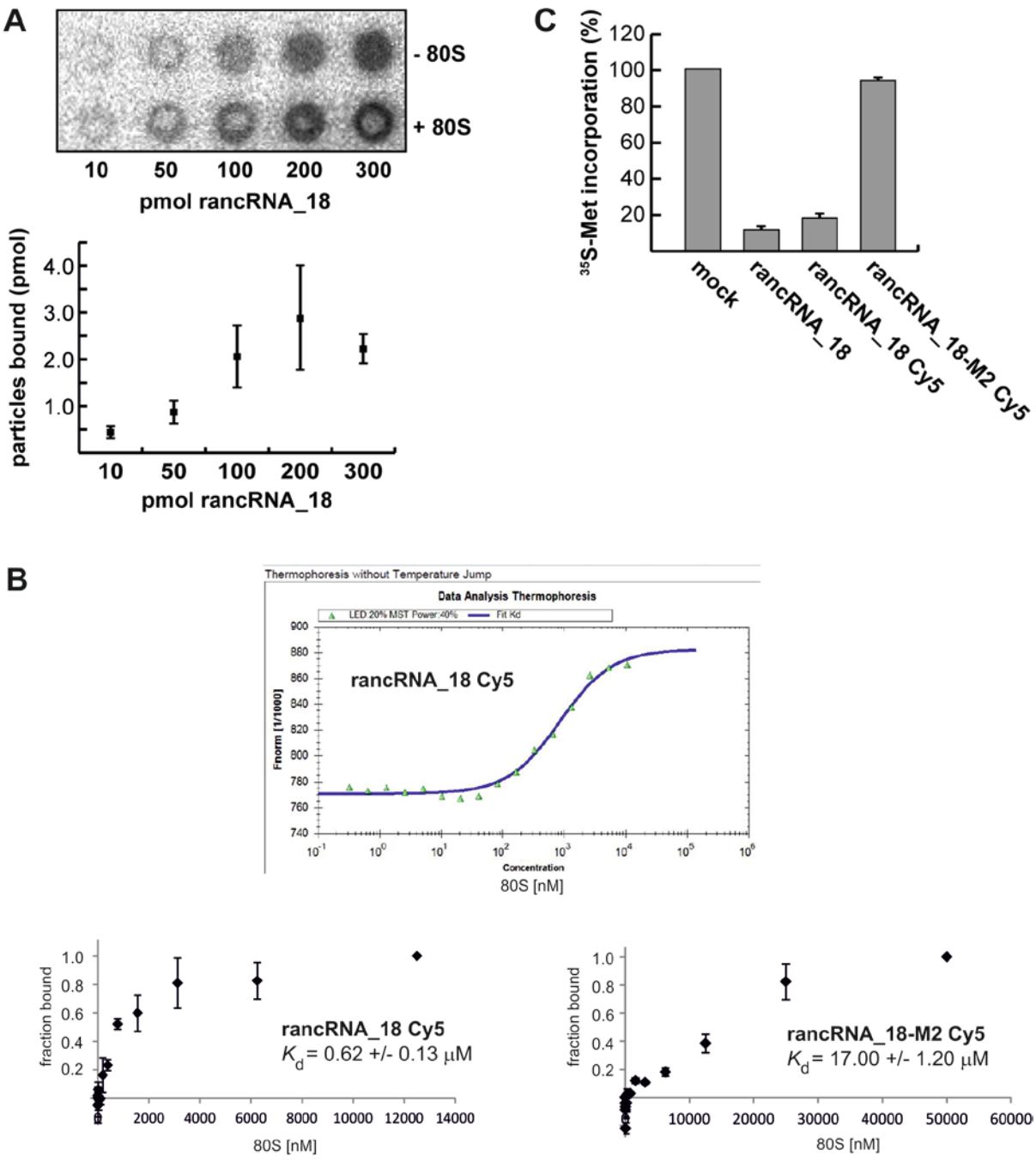

Supplementary Figure S1: Biochemical characterization of rancRNA_18.

(A) Dot blot filter binding analysis for increasing amounts of ^{32}P-labeled rancRNA_18 with 5 pmol 80S ribosomes. Samples without ribosomes (- 80S) served as background controls. n = 3; mean ± SD**. (B)** The interaction of 80S ribosomes with rancRNA_18 was investigated using microscale thermophoresis (MST). For the interaction study, fluorescently labelled (Cy5) RNA (rancRNA_18 or rancRNA_18-M2) with 80S ribosomal particles was used. The RNA concentration is kept constant while increasing amounts of 80S ribosomes are titrated. Upper part shows the raw MST data from a binding experiment using yeast 80S and

rancRNA_18 Cy5. The lower part shows the summary of three MST binding experiments with rancRNA_18 Cy5 (left) and rancRNA_18-M2 Cy5 (left). The experimentally determined K_d values for both rancRNA_18 and rancRNA_18-M2 are indicated. n = 3; mean ± SD. **(C)** The effect on global protein synthesis in yeast spheroblasts was assayed by the metabolic labelling approach. Synthetic RNA was introduced via electroporation in the yeast spheroblasts. Incorporation of ^{35}S-Met was monitored by liquid scintillation counting. A positive control without synthetic RNA was taken as 100%. The relative metabolic labeling activities of samples treated with rancRNA_18, rancRNA_18 Cy5, or rancRNA18-M2 Cy5 are shown. n = 2; mean ± SD

Supplementary Figure S2: The 49 nucleotide long 3´-extended rancRNA_18 is not functional. **(A)** Zoom into the genomic locus of rancRNA_18 (red) within the *TRM10* ORF with its 3' extension (black) is shown, resulting in the 49-mer RNA molecule. The obtained 3´-RACE sequencing data are shown. **(B)** Unlike rancRNA_18, the 3´-extended 49-mer does not affect metabolic labeling in yeast spheroplasts. Cycloheximide (CHX) was used as a negative control. Activities were normalized to the mock electroporation control. n = 3; mean ± SD; * $p < 0.05$.

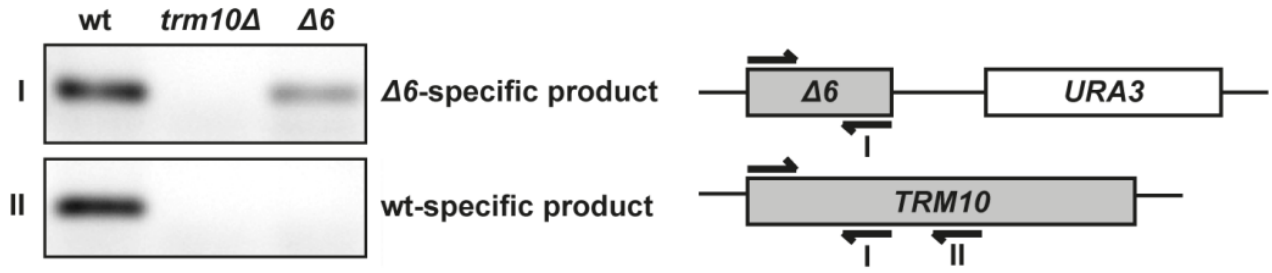

Supplementary Figure S3: Validation of the rancRNA_18 knock-in strain.

Total RNA of wt, *trm10Δ* and *Δ6* (the rancRNA_18 knock-in strain) cells was isolated and reverse transcription PCR was performed with the indicated primers. Reverse primer I amplifies wt and *Δ6* cDNA whereas reverse primer II only amplifies wt cDNA.

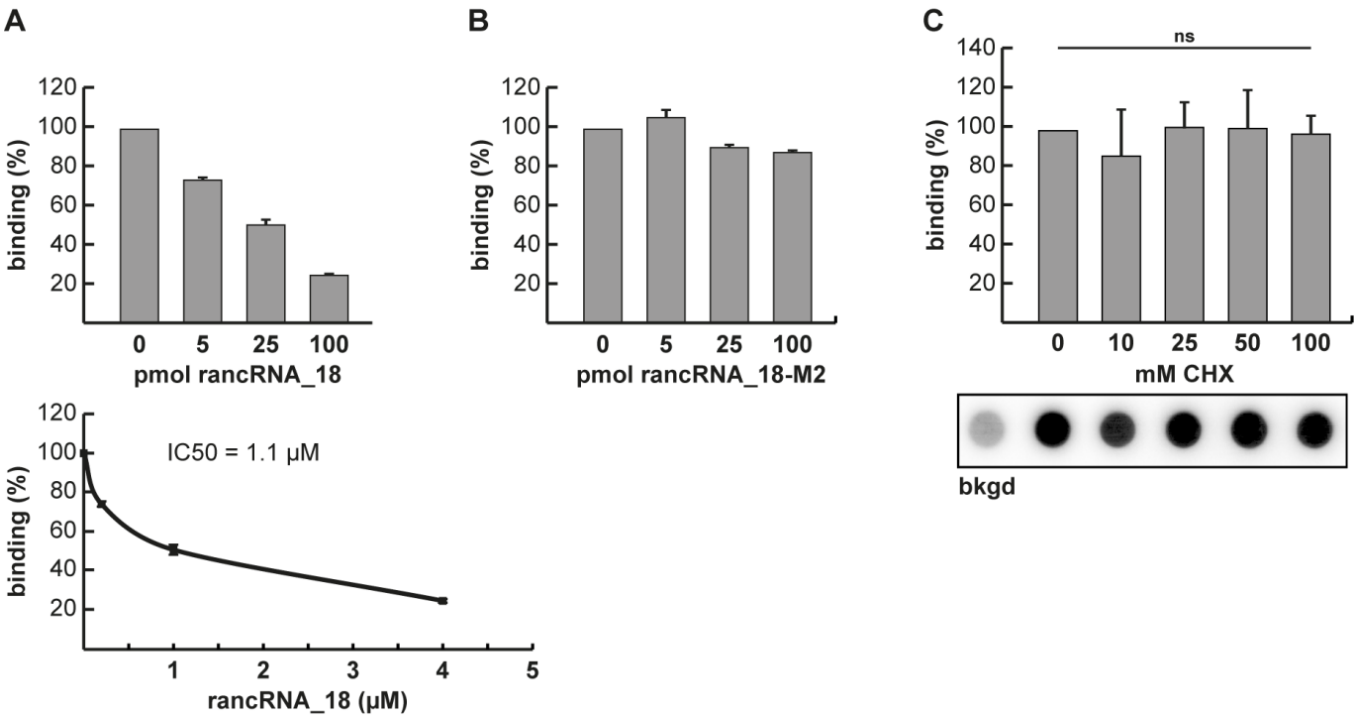

Supplementary Figure S4: rancRNA_18 can be removed from ribosomes by tRNA. (**A**) Binding competition between ^{32}P-labeled yeast bulk tRNA and increasing amounts of unlabeled rancRNA_18. tRNA binding efficiency in the absence of rancRNA_18 was taken as 100%. n = 2; mean ± SD. (**B)** As in (A) but with increasing amounts of unlabeled rancRNA_18-M2. **(C)** Binding competition between ^{32}P-labeled rancRNA_18 and increasing amounts of cycloheximide (CHX). rancRNA_18 binding in the absence of CHX was taken as 100%. n = 2; mean ± SD

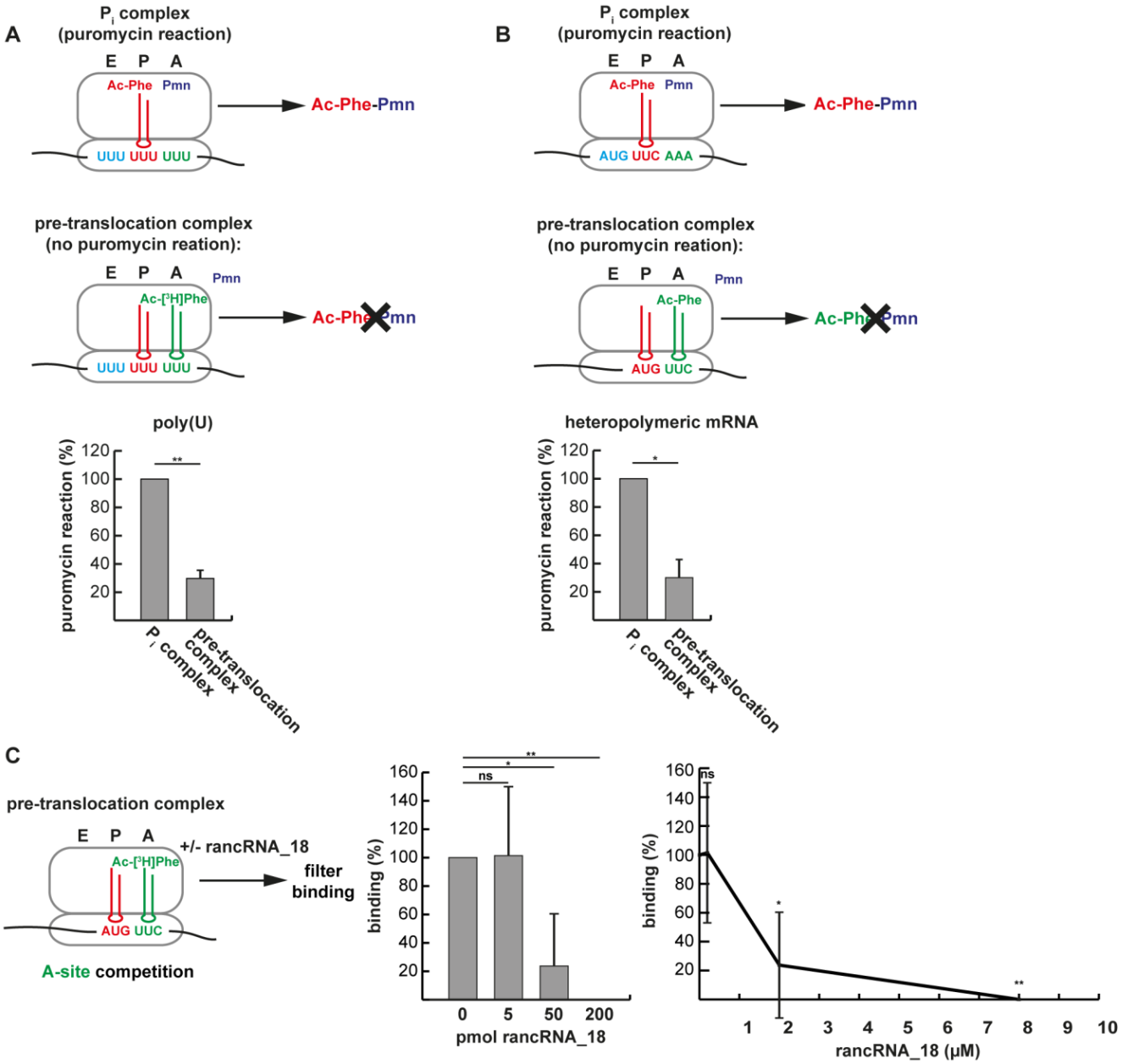

Supplementary Figure S5: Validation of ribosome/tRNA complexes with the puromycin reaction and rancRNA_18/A-tRNA binding competition. **(A)** The initiation-like complex (P_i) carrying N-acetyl-[^{3}H]Phe-tRNA^{Phe} (red) in the P-site can react with A-site bound puromycin (Pmn) to form N-acetyl-[^{3}H]Phe-Pmn. In the pre-translocational complex, when deacylated tRNA^{Phe} (red) and N-acetyl-[^{3}H]Phe-tRNA^{Phe} (green) are bound to the P- and A-sites, respectively, the peptidyl-tRNA analog (green) cannot react with Pmn. n = 3; mean ± SD; ** p < 0.01. **(B)** Same as in (A) but using a heteroploymeric mRNA carrying unique Met (AUG) and Phe (UUC) codons. n = 3; mean ± SD; * p < 0.05. **(C)** A pre-translocation complex formed on the heteroplymeric mRNA carrying deacylated tRNA^{Phe} in the P-site (red) and N-acetyl-[^{3}H]Phe-tRNA^{Phe} in the A-site (green) was used to investigate effects of unlabeled rancRNA_18 addition on tRNA occupancy. Extent of bound A-site tRNA was assessed via filter binding. n = 3; mean ± SD; ns, not significant; * p < 0.05, ** p < 0.01.

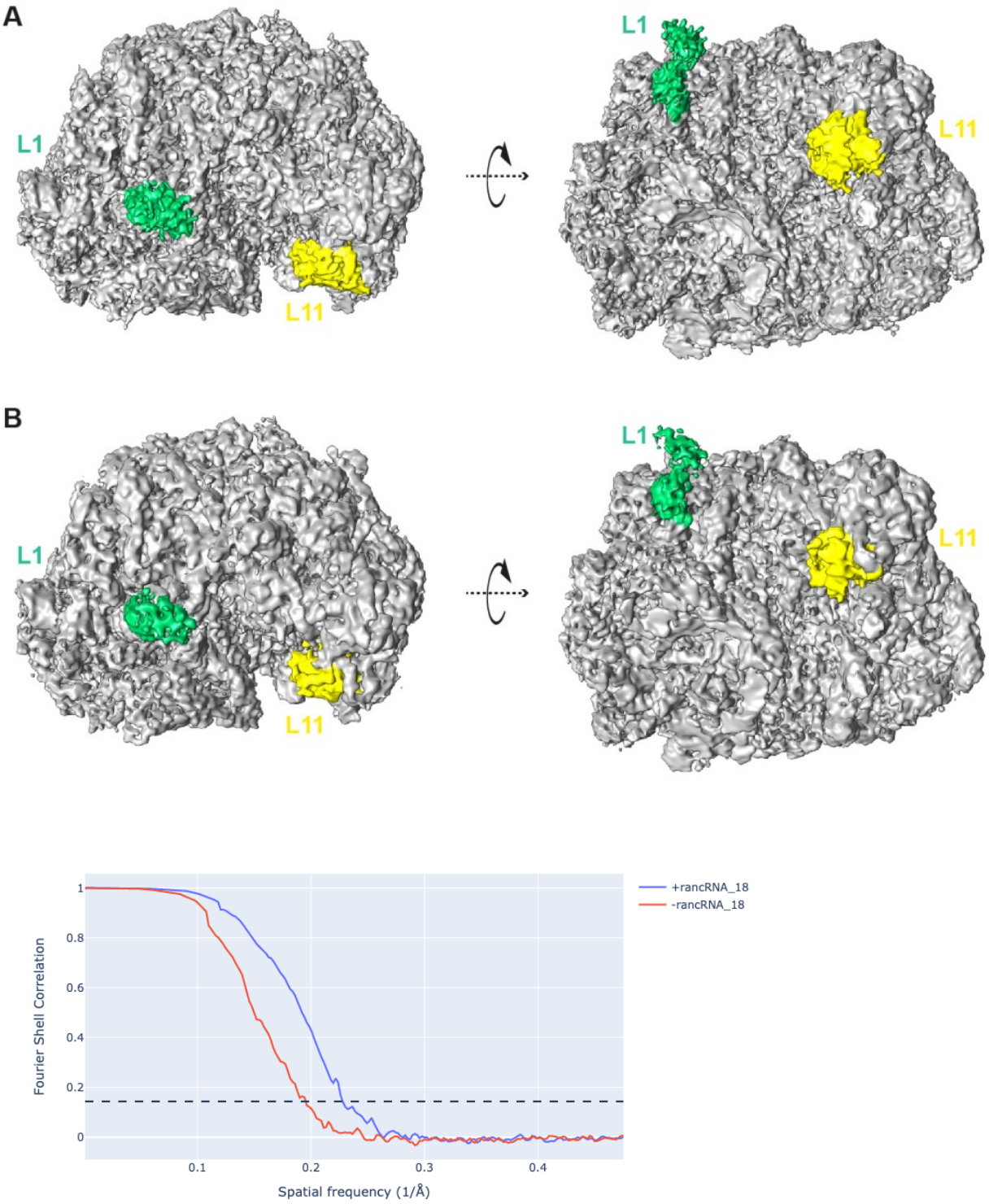

Supplementary Figure S6: Multiparticle refinement of the 60S ribosomal subunit.

(A) Cryo-EM structure of the *S. cerevisiae* 60S ribosomal subunit in the presence of rancRNA_18 at 4.4 Å resolution. **(B)** Structure of the 60S ribosomal subunit in the absence of rancRNA_18 at 5.1 Å resolution. Color code: 60S ribosomal subunit (grey), L1 stalk (green) and region of ribosomal protein L11 (uL5 according to the novel nomenclature of r-proteins) (yellow) are highlighted. Resolution estimate using FSC 0.143 criterion for -/+ rancRNA_18.

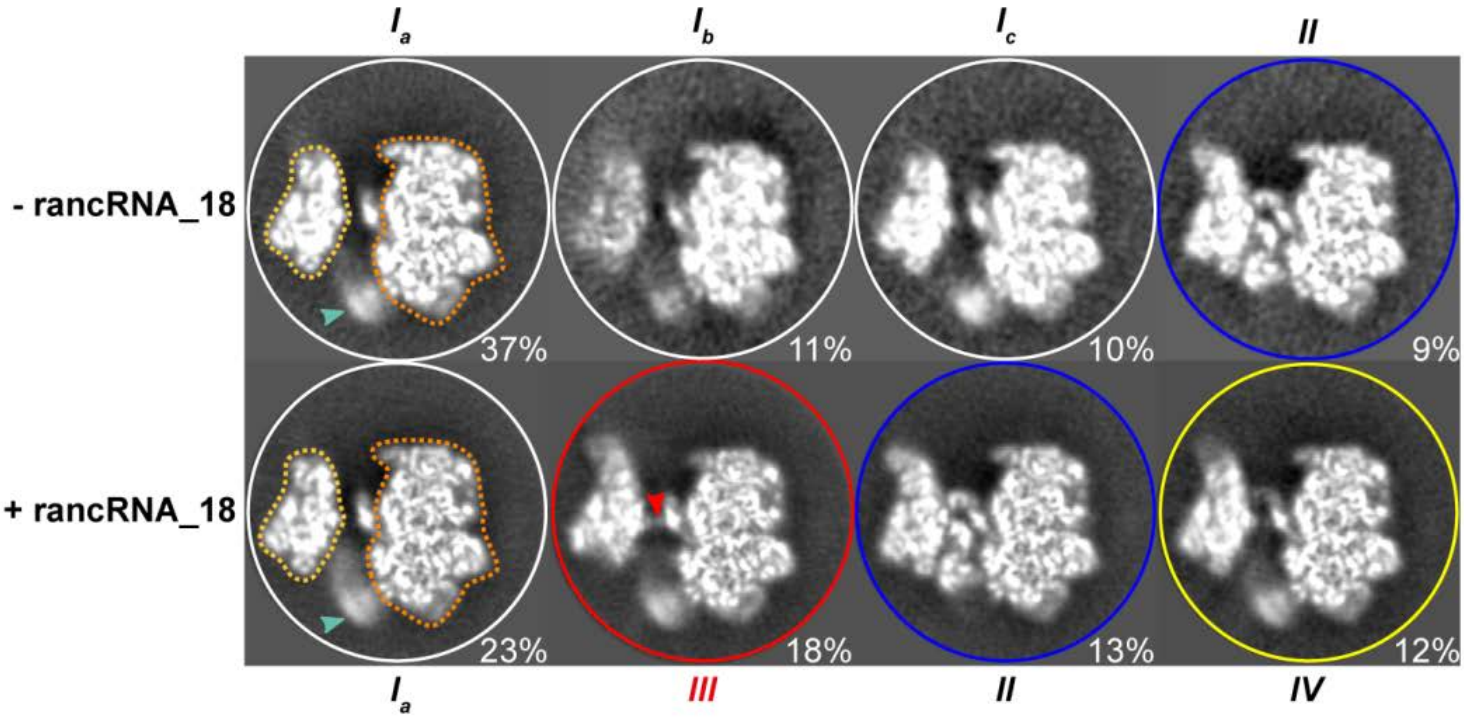

Supplementary Figure S7: 3D classification of cryo-EM images. 80S ribosomes without rancRNA_18 (upper row) showed three classes of empty particles (white frame, I_a, I_b and I_c) and a minor class containing densities for P- and E-site tRNAs (blue, *II*). Cryo-EM samples with rancRNA_18 (lower row) revealed one empty class (white, I_a), one class with densities for P- and E-site tRNAs (blue, *II*) and a class with density for only P-site tRNA (yellow, *IV*). Additionally, 18% of the particles showed a rancRNA_18-dependent extra density between the ribosomal P- and E-sites highlighted with a red arrowhead. The large (dark-orange dotted line) and small (light-orange dotted line) ribosomal subunits and the location of the L1 stalk (green arrowhead) are depicted and relative class abundances (%) are shown.

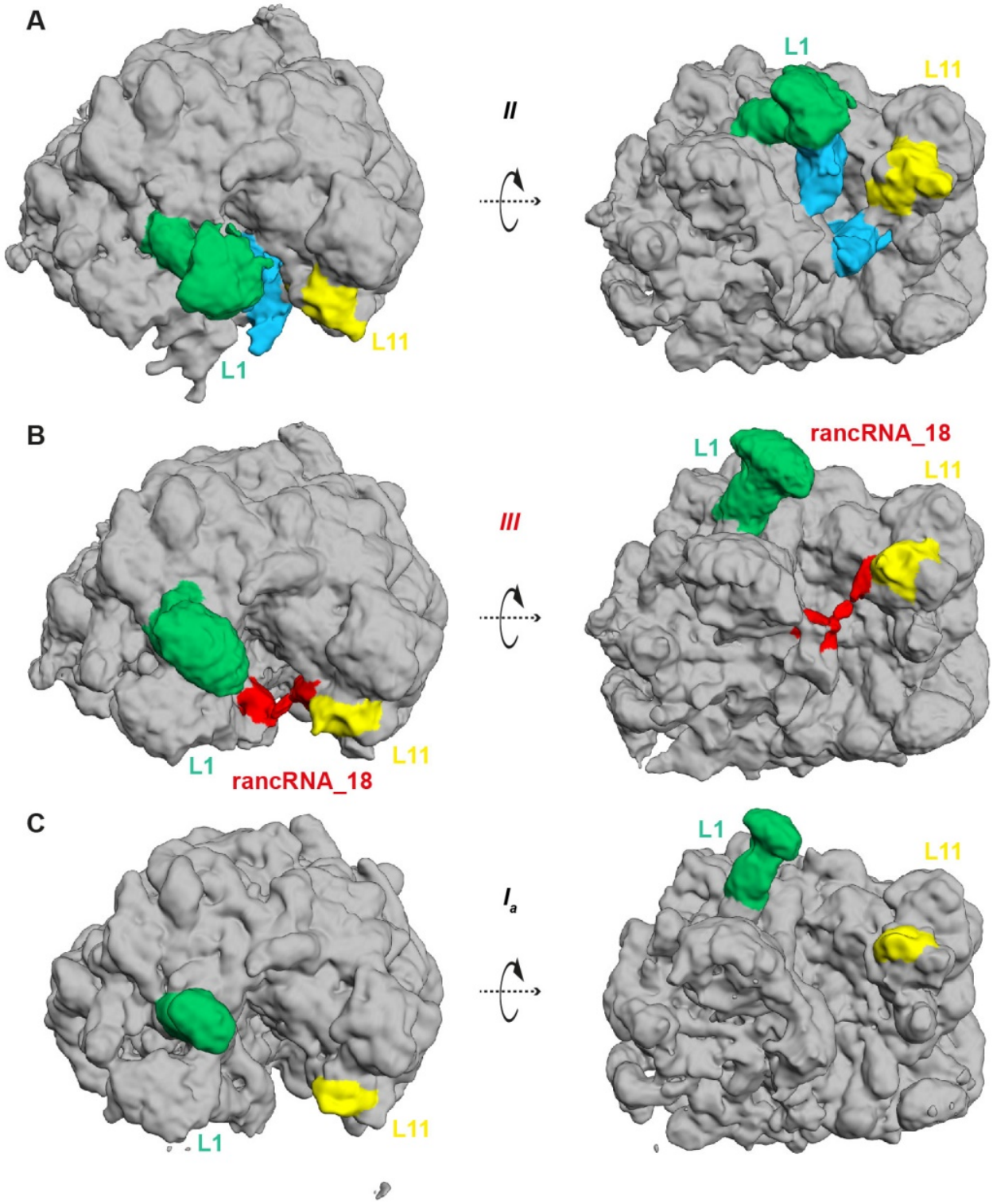

Supplementary Figure S8: RancRNA_18 binding restricts L1 stalk dynamics. Different classes of 60S subunit structures (grey) with **(A)** P- and E-site tRNA (light blue; class *II*) and the L1 stalk (green) in a fully inward position. Ribosomal protein L11 (uL5) is shown in yellow. **(B)** The rancRNA_18- dependent extra density (red; class *III*) close to the position of ribosomal protein L11 (uL5) (yellow) and the L1 stalk (green) is more ordered and in a slightly inward oriented position compared to the empty particle; **(C)** the empty ribosome (class I_a) with the L1 stalk (green) in the open conformation.

A

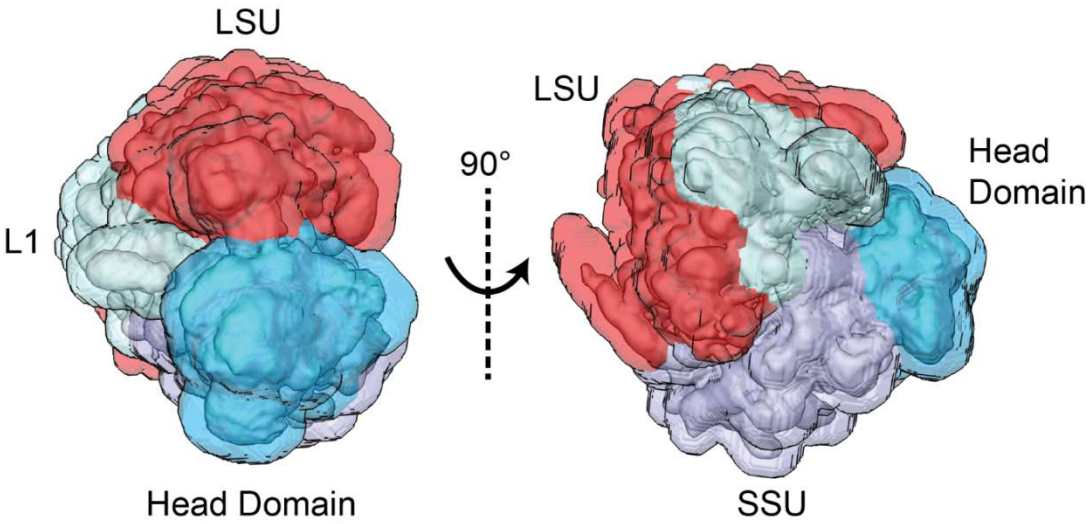

B

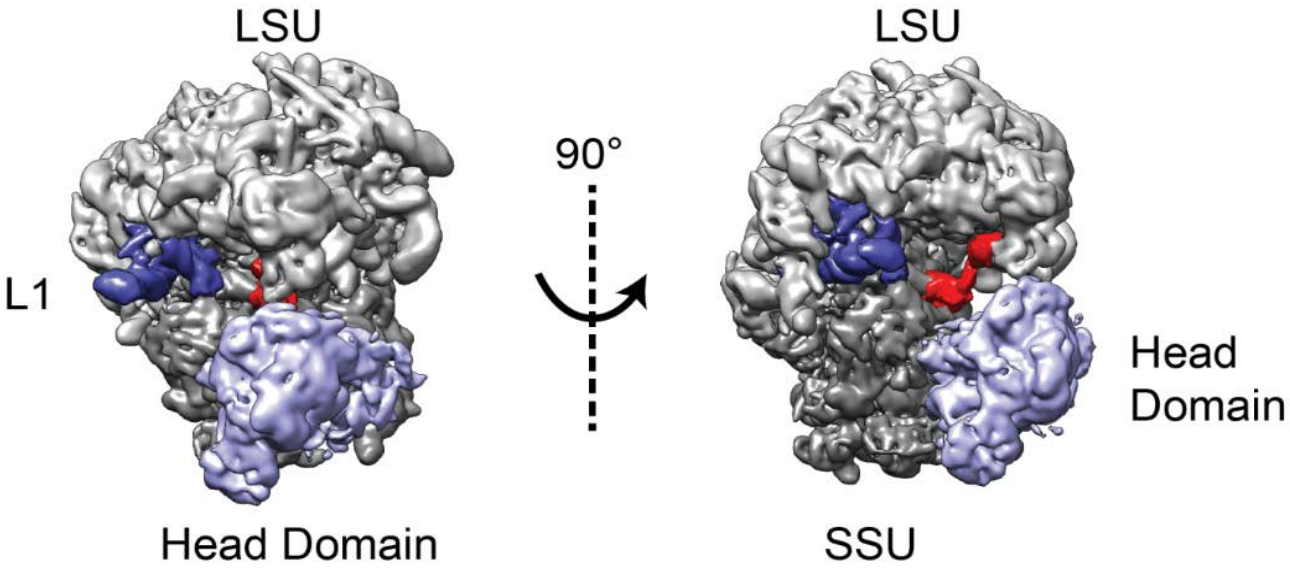

Supplementary Figure S9: (A) Illustrations of the masks used to define the four bodies for the multibody analysis of 80S ribosomes. Large ribosomal subunit (LSU) body in red, L1 in green, 40S head domain in blue and small ribosomal subunit (SSU) body in violet. The four masks are shown overlaid on the consensus refinement. **(B)** Refined 80S yeast ribosome with the position of the rancRNA_18-dependent extra density in red.

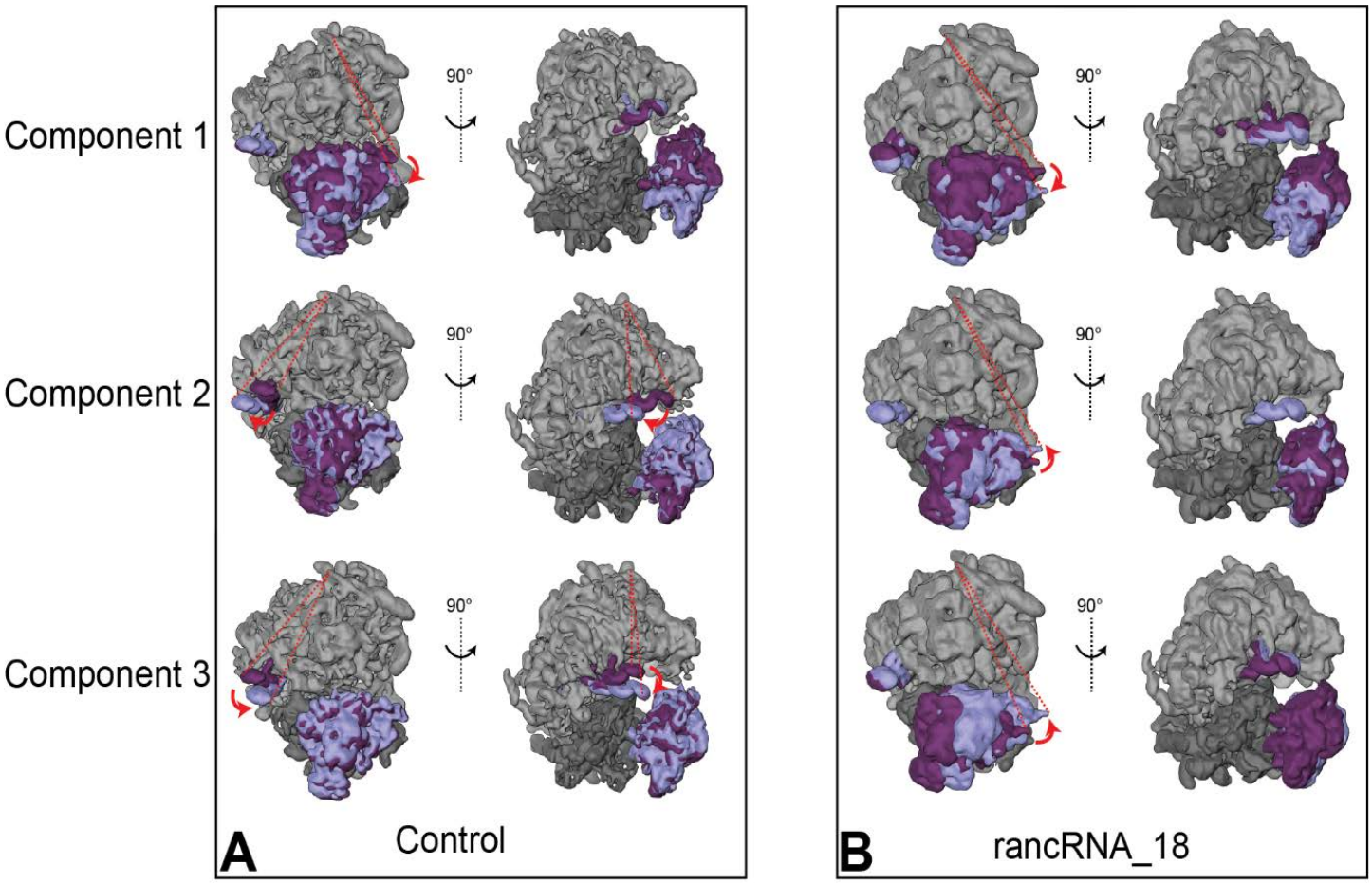

Supplementary Figure S10: Illustration of the first three components for the control sample (class I) **(A)** and ribosomal particles carrying the rancRNA_18-dependent extra density (Supplementary Figure S7; class III) **(B)** shown as the maps at the extremes. For simplicity the maps of the multibody series were docked on the large ribosomal subunit and only the L1 stalk and the small subunit head domain (both in blue) are shown for the last map. The first map is colored light gray for the large subunit, dark grey for the small subunit and violet for the flexible domains L1 stalk and the small subunit head. The coloring of the first map highlights the four masks used to define the four bodies for multibody refinement. The principal components in the control sample show the typical rotation of the head domain (Component 1) as well as movement of the L1 stalk (Components 2 and 3).. In contrast the principal components for the rancRNA_18 treated sample show only minor movement in the L1 stalk region (B).

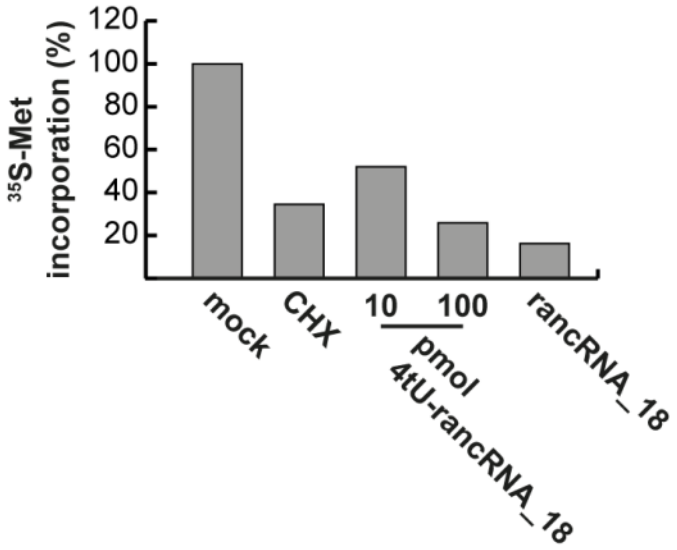

Supplementary Figure S11: *In vivo* metabolic labelling experiment shows inhibitory potential of 4tU-rancRNA_18. Different amounts of 4tU-rancRNA_18 were electroporated into yeast spheroplasts and ^{35}S-methionine incorporation was measured. Samples electroporated in the absence of synthetic RNA (mock) served as positive control. Metabolic labeling in the presence of cycloheximide (CHX) served as negative control. Electroporated 4tU-rancRNA_18 and unmodified rancRNA_18 (100 pmol) inhibited metabolic labelling to the same extent.

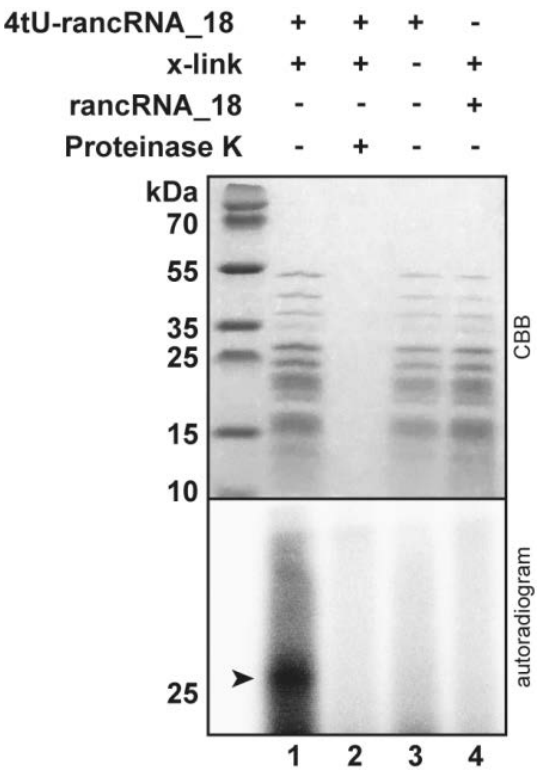

Supplementary Figure S12: RancRNA_18 cross-links to the 60S E-site region. Radioactively labeled (^{32}P)-4tU-rancRNA_18 crosslinked to r-proteins were separated on an SDS gel. The autoradiogram showed a cross-link to an r-protein in the size range of around 25 kDa (lane 1). Proteinase K treated sample (lane 2) and experiments in the presence of 4tU-rancRNA_18 without irradiation (lane 3) or in the presence of unmodified rancRNA_18 with irradiation (lane 4) served as controls. CBB, coomassie brilliant blue stain.

Supplementary Table S1

DNA Oligonucleotides

Name	5'-3' sequence
LNA*_18mer	TTCTTTTCACCTTTTCCA (*LNA residue positions were chosen according to manufacturer's suggestion)
SC_3'RACE_45mer	AGGAAAAGGTGAAAAGAACA
Sc_ivt_49mer_fwd	GGATCCTAATACGACTCACTATAGGAGGAAAAGGTGAAAAGAACACCACCTTTACCGCCT
Sc_ivt_49mer_rev	ATGCCTTCTGGCACAGGCGGTAAAGGTGGTGTTC
Sc_LEU2_rev	TTAAGCAAGGATTTTCTTAACTTCTT
Sc_LEU2_T7_fwd	GGATCCTAATACGACTCACTATAGGGAGAATGTCTGCCCCTAAGAAGATC
Sc_TL mutant_fwd	TGTGCCGAAAGGCATGTCTAAAAAGCAATGGAAAAA
Sc_TL mutant_rev	CATGCCTTTCGGCACAGGCGGTAAAGGTGGT
Trm10_knock_in_fwd	CTCGATACAACATTACGTTTTGTAAATTTATCACAAAAGCTTACCATCTTTAGCGATTTGCTGAAGT
Trm10_knock_in_rev	CCGCATTGTATTTGGCTTTATT
TRM10_short_T7_fwd	GGATCCTAATACGACTCACTATAGGGAGATTACCATCTTTAGCGATTTGCTGAAGT
Ura_fwd	ATGTCGAAAGCTACATATAAGGAA
Ura_rev chrI: 18880 – 18840	AGCAGTCGAAAACTTTTGATGCACCAAACACCGTTCTTGA TTAGTTTTGCTGGCCGCATCTTCT
Sc_rnt1_sub.fwd	GGATCCTAATACGACTCACTATAGGGATGTCCAATGATGAGATAAACCAGAACG
Sc_rnt1_sub.rev	TCCATTGCTTTTTAGACATGCCTTCT
rnt1_control	GGCGCCATGCCATGCCATGGACTCATGACATGACATGACGCCTATAGTGAGTCGTAT
stem_mut_rev	TTCTGGCACAGGCGGTCCCGGTGGTG
stem_mut_fwd	AGGAAAAGGTGAAAAGAACACCACCGGGACCGCCT
pe_1_PTC1	TAGTGGGTGAACAATCCAA
pe_2_PTC2	ACCGAATTCTGCTTCGGTAT
pe_3_h76	AAGTAAAATAACGTTAAAA
pe_4_h77	AAAAGTAGTGGTATTTCA
pe_5_h83	AAAATCAAGGGGGCTTTT
pe_6_h79	CCGCTTCATTGAATAAC
pe_7_h89	GCTATGAACGCTTGGCTG
pe_8_h74	ACTAGAGTCAAGCTCAACAG
pe_9_PTC3	GGTATGATAGGAAGAGCC
pe_10_h86	TTTCATGGTTTGTATTCA
pe_11_h76.2	TAAGTAAAGAAACTATAAAG
pe_12_h86.2	CACACTGAAAATCAAAAT
pe_13_5S	CGGTCAGGCTCTACCAGC
pe_14_h88	GGTAACTTTTCTGGCACC
pe_15_h69	AATCCATTCATGCGCGTCA
pe_16_h68	ACTCCCGCCGTTTACCCG
pe_17_h82	AGATTTCTGTTCTCCATGA
pe_18_h93	TCAGTAGGGTAAAACTAA
TRM10_BamHI_1 (short 2)	TATATAGGATCCTTTCAGAGTAGTTTCAAACCTTTGC
TRM10_BamHI_2 (short 8)	TATATAGGATCCCCTTCTGGCACAGGCGGTAAAGGTGG
TRM10_BamHI_3 (short 9)	TATATAGGATCCGGTAAAGGTGGTGTTCTTTTCAC
TRM10_BamHI_4_rev (short 3)	TATATAGGATCCTTCGCCCTTCTATTCGCGGAGTATG
TRM10_BamHI_short 5 (short 4)	TATATAGGATCCCTCTCTAATCAATTCCTGCGGGACC
TRM10_BamHI_short 6 (short 5)	TATATAGGATCCTGGCGAAGTCTCCTTCTTCTTTACAC
TRM10_BamHI_short7 (short 6)	TATATAGGATCCCCGCATTGTATTTGGCTTTATT
TRM10_BamHI_short8 (short 7)	TATATAGGATCCACACATTTTTTTCCATTG
URA3 K.I. fwd	gtcttgatcgacacataattcgaatgGTTTTATTTAGGTTCTATCGAGG
URA3KI_ki_ChrVrev	caatcatcatccatcgtctaatattgtaaactagtataccatcatatGATCCCAATACAACAGATCAC
TRM10_ki_ChrVfwd	caattaaaacattatattaagattattgatttgccttttaagggtccTTACCATCTTTAGCGATTTGCTGAAGT
TRM10_ki_rev	cattcgaattatgtgtcgatcaagacCCGCATTGTATTTGGCTTTATT
ChrV fwd	CAATTAAAACATTATATTAAGATTATTG
ChrV rev	CAATCATCATCCATCGTC

RNA oligonucleotides

Name	5'-3' sequence
rancRNA_18	AGGAAAAGGUGAAAAGAA
rancRNA_18-M2	AGGAGAAAGUUAAAAGAA
rancRNA_18-M2-Cy5*	AGGAGAAAGUUAAAAGAA*
4tU-rancRNA_18	AGGAAAAGG-4tU-GAAAAG-4tU-A

Supplementary Table S2

sample	pocket	component	variance explained [%]	movement	displacement range [Å]	weighted average displacement [Å]
Control	empty	1	10.3	head rotation	35.0	5.6
		2	8.4	L1 swing in-out	42.0	6.8
		3	8.3	L1 swing up-down	28.0	4.6
RancRNA-18	empty	1	11.6	head rotation 1	26.0	4.7
		2	8.9	L1 swing in-out	28.0	5.0
		3	8.8	head rotation 2	24.0	4.6
	occupied	1	11.1	head rotation 1	24.0	4.0
				L1 minor swing up-down	7.4	1.2
		2	9.5	head rotation 2	24.0	3.7
				L1 minor swing up-down	6.4	1.0
		3	8.1	head rotation 3	28.0	4.5

Supplementary Movie S1: Positioning of the reconstructed densities along the first three vectors showing the principal movements present in the different classes. Empty class from the control data set features large movements of the L1 stalk and the head domain while the rancRNA_18 data set features minor, restricted L1 stalk movements. Movie was generated with chimera volume series tool and edited in Camtasia.